A moving horizon state-estimation approach for switching system of a Single-Link Flexible Joint Manipulator

Lara Candido Alvim*, Leonardo Dias Pereira*, Elias Dias Rossi Lopes and Helon Vicente Hultmann Ayala***

**Department of Mechanical Engineering, Pontifical Catholic University of Rio de Janeiro (PUC-Rio) Marques de Sao Vicente, 225 - Gávea, Zip code 22453-900, Rio de Janeiro, RJ, Brazil (e-mails: llaracalvim@gmail.com, leopereiradias@yahoo.com.br, helon@puc-rio.br)*

***Department of Mechanical Engineering, Military Institute of Engineering (IME) General Tibúrcio Sq, 80 - Urca, Zip code 22290-270, Rio de Janeiro, RJ, Brazil (e-mail: eliasrossi@ime.eb.br)*

Abstract: In recent decades, the increased use of robotic manipulators in the industrial environment has increasingly impacted the human-robot interaction and the safety performance during this interaction. Consequently, control methods that can predict contact, control force, or trajectory to avoid damage during collision become required. This paper considers mode and state estimation for detecting contact in a single-link flexible joint manipulator using the moving horizon estimation (MHE) approach. This method was addressed by employing a least-squares optimization problem, solved for each instant of time to select the best estimation of the system behavior. First, the main aspects of the method have been presented, then the effectiveness of the proposed approach was demonstrated through simulation results, comparing the solution for the real system and the estimate.

Keywords: Moving horizon estimation (MHE); State estimation; Mode estimation; Switching systems; Least-square optimization; Robotic manipulator; Flexible joint.

1. INTRODUCTION

The use of robotic manipulators and their range of possible applications has increased in recent decades. The impact of this increase is not only in the research areas but also in the industry, and it raises an essential issue that is human-robot collaboration. A current challenge in robotics and one of the most concerning issues in the industrial environment is the detection and response of robots to unexpected collisions, as it is related to safety in human-robot interaction (Li et al. 2018, Jung et al. 2014).

Several methods for detecting and reducing the occurrence of collisions, for example Ullah et al. (2021), Raza et al. (2019), Kamel et al. (2019), Chen et al. (2018), Li et al. (2018), Kouris et al. (2018), Vorndamme et al. (2017), Dimeas et al. (2015, Jung et al. (2014), and Song et al. (2011), link this problem to switching systems controls, dividing the research into two topics, force and trajectory control. The wide variety of practical applications of switching or multimode systems makes the modeling of these systems a relevant issue. Consequently, this has become a more discussed topic that brings the development of new control and analysis methods. Among a set of analysis properties that can be used, the observation of modes plays a crucial role in determining whether or not the outputs of a system can be identified and differentiated (Baglietto et al. 2012).

In order to improve the accuracy of mode-observability of systems, some papers have investigated the Moving Horizon Estimation (MHE) approach (Guo and Huang, 2013, Alessandri et al. 2005). The Moving Horizon Estimation (MHE) has emerged as a powerful technique for tackling the problem of estimating the state of a dynamic system in the presence of nonlinearities and disturbances (Alessandri et al. 2010). The main idea behind the MHE method is minimizing an estimation cost function, defined on a sliding window (Nocedal et al. 2006), states that the least-square problems measure the discrepancy between the model and the observed behavior of the system, and select values for the parameters that best match the model to the data by minimizing the objective function.

In this work, we extend the results of Baglietto et al. (2012) by considering another practical application of the mode-observability properties for nonlinear switching systems with noisy-corrupted mode observations. More specifically, a single link flexible joint manipulator is modeled to have some specific dynamic tasks (that define the modes) to be done. With unknown noise corrupting output measurements and, consequently, the mode observations, the design of a nonlinear discrete-time switching system with a trusted estimator is a challenging problem. In order to achieve a viable approach for such a system, we use the MHE approach for switching systems, where the mode and states can vary in unpredictable ways. Finally, the mode and states

estimation is presented with a rigorous analytical framework that focuses on: (i) surveilling and comparing along the time the real and estimated continuous-time state and discrete-time modes; (ii) deriving mode estimation performance index; (iii) deriving the state estimation performance index; (iv) deriving statistical analysis for a batch of cases.

The note is organized as follows. The problem of MHE for discrete-time nonlinear switching systems is drawn in Section 2, where we state the continuous time switching system, the general moving horizon state estimation, and we also present the algorithm of the moving horizon state estimation for switching systems. The single link flexible joint dynamical model is stated in Section 3. In Section 4, the focus is on the simulation results of the proposed case study. Lastly, Section 5 concludes this note and prospects future work.

2. MOVING HORIZON STATE ESTIMATION FOR SWITCHING SYSTEMS

In this section, some preliminary concepts related to switching systems and moving horizon state estimation are presented.

2.1 Continuous-Time Nonlinear Switching Systems

A switched system is a dynamical system that consists of a finite number of subsystems described by differential or difference equations and a logical rule that orchestrates switching between these subsystems (Lin et al., 2007).

Nonlinear Switching Systems are typically characterized as a set of nonlinear dynamical systems, where each subsystem is activated by a discrete-value variable known as a switching signal, Du et al. (2021). According to Liberzon (2003) and Du et al. (2021), the continuous-time switched nonlinear system is defined as follows

$$\dot{x}(t) = f_{\sigma_t}(x_t, u_t) \tag{1}$$

where $x \in \mathbb{R}^n$, is the continuous state vector, $u \in \mathbb{R}^n$ is the input vector. $\sigma_t \in \{1, 2, ..., m\}$ is a piecewise constant function (switching signal) that determines the sequence of mode activations between the n subsystems.

2.2 Moving Horizon State Estimation (MHSE)

The MHSE problem, also known as finite-memory, receding-horizon, or sliding-window estimation, consists of using a set of most recent information within a time interval to solve an optimization problem that estimates the dynamic states of a system. The estimator is derived by minimizing a quadratic cost function and, accordingly to Alessandri et al. (2005) two contributions are made up: the first term is a weighted term penalizing the distance of the current estimated state from its prediction (both computed at the beginning of the sliding window); the second is the usual prediction error computed on the basis of the most recent measures.

Let the system be modeled by the following nonlinear discrete-time system

$$x_{t+1} = f(x_t, u_t) + \varepsilon_t \tag{2a}$$
$$y_t = h(x_t) + \eta_t \tag{2b}$$

where $t \in \mathbb{Z}_+ = \{0, 1, ..., \}$ is the time instant; $x_t \in \mathcal{X} \subset \mathbb{R}^n$ is the state vector (the initial state x_0 is unknown); $u_t \in \mathcal{U} \subset \mathbb{R}^m$ is the input signal vector; $\varepsilon_t \in \subset \mathbb{R}^n$ is the system noise vector; $y_t \in \mathbb{R}^p$ is the output/observation vector; and $\eta_t \in \mathcal{V} \subset \mathbb{R}^n$ is the random measurement noise vector. The statistics of the random variables x_0, η_t are assumed to be unknown deterministic variables with unavailable statistics. Functions f and h are nonlinear.

In this paper, the estimates are based on data obtained according to a receding-horizon strategy where the observation window is composed of $(N+1)$ measurements for a time interval $[t-N, t]$ with $t \geq N$.

The objective of the MHSE is to find the estimates $\hat{x}_{t|t}$ of x_t at time t on the basis of $\{y_{t-N}, ..., y_t, u_{t-N}, ..., u_t\}$ and of the "prediction" $\bar{x}_{t-N}$ of the state x_{t-N}. The estimates $\{\hat{x}_{t-N|t}, ... \hat{x}_{t|t}\}$ of $\{x_{t-N}, ..., x_t\}$ are calculated at time $t = N, N+1, ...$ by minimizing a least-squares cost function as follows

$$J_t = \mu|\hat{x}_{t-N|t} - \bar{x}_{t-N}|^2 + \sum_{i=t-N}^{t} |y_i - h(\hat{x}_{i|t}, u_i)|^2 \tag{3}$$

where μ is a nonnegative weighting term by which we express our belief in the prediction $\bar{x}_{t-N}$. The vector $\bar{x}_0$ denotes an *a priori* prediction of x_0.

2.3 Moving Horizon State Estimation for Switching Systems

The mode estimation method is a strategy that can be suitable for systems in which modes vary unpredictably over time due to the possibility of using a fixed observation window. This performance depends on an *a priori* estimation of all the continuous states of the systems.

Based on the returned value of an objective function for each estimate within a moving horizon window, the discrete state, i.e., the active mode of the system, is estimated (Ayala, 2012).

Now, let us define the switched nonlinear discrete-time equation as a combination of the switched nonlinear equation with the nonlinear discrete-time equations

$$x_{t+1} = f_{\sigma_t}(x_t, u_t) + \varepsilon_t \tag{4a}$$
$$y_t = h_{\sigma_t}(x_t) + \eta_t \tag{4b}$$

The state estimation procedure of a nonlinear switching system within a moving-horizon can be formulated as stated by Ayala (2012), at any instant of time $t = N, N+1, \ldots$, based on the recent information vector I_t and in a previously known prediction of the initial conditions $\bar{x}_{t-N}$, deduce the estimation of the mode $\hat{\sigma}$ and of the state vectors $\hat{x}_{t-N,t|t}$.

To infer $\hat{\sigma}$ and $\hat{x}_{t-N|t}$, on basis of I_t and $\bar{x}_{t-N}$, by resorting to a least-square approach, one can consider the following moving-horizon strategy (Baglietto et. al., 2012; Ayala, 2012)

$$\hat{\sigma}_t, \hat{x}_{t-N|t} \in argmin_{\hat{\sigma}_t \in M, \hat{x}_{t-N|t} \in \chi} J(\hat{x}_{t-N|t}, \bar{x}_{t-N}, \hat{\sigma}_t, I_t) \quad (5)$$

where

$$\hat{x}_{k+1|t} = f_{\hat{\sigma}_t}(\hat{x}_{k|t}, u_k), k = t-N, ..., t-1 \quad (6)$$

and

$$\bar{x}_{t-N|t} = f_{\hat{\sigma}_{t-N-1}}(\hat{x}_{t-N-1|t-1}, u_{t-N-1}), \quad t = N+1, N+2, \ldots \quad (7)$$

The cost function is defined as

$$J(\hat{x}_{t-N|t}, \bar{x}_{t-N}, \hat{\sigma}_t, I_t) = \mu \parallel \hat{x}_{t-N|t} - \bar{x}_{t-N} \parallel^2 + \parallel y_{t-N|t} - F_{\hat{\sigma}t}(\hat{x}_{t-N|t}, u_{t-N,t-1}, N) \parallel^2 \quad (8)$$

The optimal estimate made at time t for each sequence of modes $i \in M$ is denoted by (9)

$$\hat{x}^i_{t-N|t} \in argmin_{\hat{x}^i_{t-N|t} \in \chi} J(\hat{x}^i_{t-N|t}, \bar{x}_{t-N}, i, I_t), i = 1, 2, ..., m \quad (9)$$

and the optimal associated cost is denoted by (10)

$$J(\hat{x}^i_{t-N|t}, \bar{x}_{t-N}, i, I_t) = \mu \parallel \hat{x}^i_{t-N} - \bar{x}_{t-N} \parallel^2 + + \parallel y_{t-N,t} - F_{\hat{\sigma}_t}(\hat{x}^i_{t-N|t}, u_{t-N,t-1}, N) \parallel^2 \quad (10)$$

Summing up, the mode estimation scheme takes the form of the pseudocode stated by Ayala (2012) and shown in Algorithm 1.

Algorithm 1. State Estimation of Nonlinear Switching Systems

1: **begin**
2: Given $\mathcal{M} = \{1, 2, \ldots, m\}$, $\bar{x}_0$
3: $t = N$
4: **while** Stopping criteria is not met **do**
5: $J\left(\hat{x}^{i^o}_{t-N|t}, \bar{x}_{t-N}, i^o, I_t\right) = \infty$
6: Compute the optimal estimates $\hat{\sigma}_t$ and $\hat{x}_{t-N|t}$ with respect to (Eq X):
7: **for** $i = 1, 2, ..., m$ **do**
8: Perform the optimization procedure:
9: $\hat{x}^i_{t-N|t} = arg\ min_{\hat{x}^i_{t-N|t}} \epsilon\, x\, J\left(\hat{x}^i_{t-N|t}, \bar{x}_{t-N}, i, I_t\right)$
10: Compare the i-th mode cost function with the best found so far
11: **if** $J\left(\hat{x}^i_{t-N|t}, \bar{x}_{t-N}, i, I_t\right) < J\left(\hat{x}^{i^0}_{t-N|t}, \bar{x}_{t-N}, i^0, I_t\right)$ **then**
12: $i^0 = i$
13: $\hat{x}^{i^0}_{t-N|t} = \hat{x}^i_{t-N|t}$
14: $J\left(\hat{x}^{i^0}_{t-N|t}, \bar{x}_{t-N}, i^0, I_t\right) = J\left(\hat{x}^i_{t-N|t}, \bar{x}_{t-N}, i, I_t\right)$
15: **end if**
16: **end for**
17: Output the estimates $\hat{\sigma}_t$ and $\hat{x}_{t-N|t}$:
18: $\hat{\sigma}_t = i^0$
19: $\hat{x}_{t-N|t} = \hat{x}^{i^0}_{t-N|t}$
20: **for** $k = t-N, \ldots, t-1$ **do**
21: $\hat{x}_{k+1|t} = f_{\hat{\sigma}_t}(\hat{x}_{k|t}, u_k)$
22: **end for**
23: Propagate the prediction $\bar{x}_{t-N+1}$:
24: $\bar{x}_{t-N+1} = f_{\hat{\sigma}_{t-N}}(\hat{x}_{t-N}, u_{t-N})$
25: $t = t + 1$
26: **end while**
27: **end**

2.4 Performance Indexes

For the sake of comparison, let us consider the mode performance index given by the percentage of correct mode estimation at any time of the observation window:

$$C_{\sigma_t|\hat{\sigma}_t} = \left(1 - \left|\frac{\hat{\sigma}_t - \sigma_t}{\sigma_t}\right|\right) \times 100\% \quad (11)$$

where σ_t is the real mode observed, $\hat{\sigma}_t$ is the estimated mode observed, and $C_{\sigma_t|\hat{\sigma}_t}$ is the percentage of correct mode estimation.

We also define the state performance index given by the Root Mean Square Error (RMSE) at the beginning $[t-N, t]$ and the end $[t, t]$ of the observation window as

$$RMSE_t := \left(\sum_{k=1}^{K} \frac{\left\|e^k_t\right\|^2}{K}\right)^{\frac{1}{2}}, k = 0, 1, .., K - \quad (12)$$

e_t^k is the estimation error of continuous state at discrete time k in the kth simulation run. K is the number of simulation runs. N is the simulation horizon.

3. CASE STUDY

In the present section, we describe the dynamical modeling of a single-link flexible joint manipulator for which a two-modes nonlinear switching autonomous system is considered. The two modes correspond to (1) free dynamics and (2) contact model dynamics.

3.1 Dynamical Model

The single-link flexible joint manipulator (SLFJM) consists of a link driven by a motor and an elastic flexible joint in between. The angular position of the link and of the motor are measured by angular sensors as shown in Fig. 1.

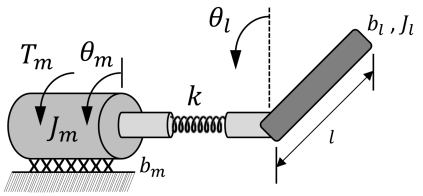

Fig. 1 Single-Link Flexible Joint Manipulator (SLFJM): Free Model

Based on the Euler Lagrange Derivations, the equations of motion of the SLFJM are described as

$$J_m\ddot{\theta}_m + b_m\dot{\theta}_m - k(\theta_l - \theta_m) = T_m \quad (13a)$$
$$J_l\ddot{\theta}_l + k(\theta_l - \theta_m) + mglsin(\theta_l) = 0 \quad (13b)$$

where, T_m is the motor torque, J_m and J_l are the motor and link inertia, b_m is the motor viscous friction coefficient, θ_m, $\dot{\theta}_m$, and $\ddot{\theta}_m$ are the angular position, velocity, and acceleration of the motor, θ_l and, $\ddot{\theta}_l$ are the angular position and acceleration of the link, k is the stiffness constant of the spring which represents the flexible joint in the model, m is the link mass, g is gravity acceleration and l is the link length.

The manipulator described in (13a) and (13b), may be represented by a discrete-time nonlinear state space model on the form of (2a) and (2b), where the continuous states are defined as $x_1 = \theta_m$, $x_2 = \dot{\theta}_m$, $x_3 = \theta_l$, $x_4 = \dot{\theta}_l$, the input variable as $u = T_m$, and the system and measurement equations are defined, respectively, as

$$f(x_t, u_t) = \begin{bmatrix} x_2 \\ -\frac{1}{J_m}k(x_1 - x_3) - \frac{1}{J_m}b_m x_2 + \frac{1}{J_m}k_t u \\ x_4 \\ \frac{1}{J_l}k(x_1 - x_3) - \frac{1}{J_l}mglsin(x_3) \end{bmatrix} \quad (14)$$

$$h(x_t) = \begin{bmatrix} x_1 \\ x_2 \\ x_3 \\ x_4 \end{bmatrix} \quad (15)$$

3.2 Contact Modeling

Now, let us consider the presence of a fault in the previously described system due to extra abnormal friction in the contact between the link and a surface. Within this approach, one mode is defined as the nominal condition, while the other mode is used to model the fault of the system, as the SLFJM schematic diagram shows in Fig. 2.

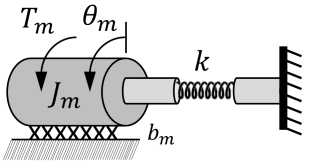

Fig. 2 Single-Link Flexible Joint Manipulator: Contact Model

The abnormal friction in the contact between the link and a surface prevents the link displacement.

For the case of the SLFJM, the fault system may be represented by the nonlinear switching system in the form of equations (4a) and (4b) where the discrete state defines the nominal system and its faulty condition. Let the set of possible modes be $\sigma_t \in \mathcal{M} = \{1, 2\}$, where $\sigma_t = 1$ correspond to the nominal condition, and $\sigma_t = 2$ the pre-defined fault (contact model). Accordingly, the system equations have the matrix form

$$f_1(x_t, u_t) = \begin{bmatrix} x_2 \\ -\frac{1}{J_m}k(x_1 - x_3) - \frac{1}{J_m}b_m x_2 + \frac{1}{J_m}k_t u \\ x_4 \\ \frac{1}{J_l}k(x_1 - x_3) - \frac{1}{J_l}mglsin(x_3) \end{bmatrix} \quad (16)$$

$$f_2(x_t, u_t) = \begin{bmatrix} x_2 \\ -\frac{1}{J_m}k(x_1 - x_3) - \frac{1}{J_m}b_m x_2 + \frac{1}{J_m}k_t u \\ 0 \\ 0 \end{bmatrix} \quad (17)$$

Note that the nominal condition is modeled with the nominal nonlinear dynamical model. However, some fault importance state are modeled with constant value that makes the states x_3 and x_4 null. This indicates that the link position and the link velocity is stopped.

Finally, by applying a mode estimation algorithm to the continuous states of the system, it is possible to estimate the switching between them and approximate their real value. If the switching sequence belongs to the set of modes, we can adopt a moving horizon approach to solve the problem.

4. SIMULATION MODEL DESCRIPTION

According to Zhang et. al (2010), and Fan and Arcak (2003), suitable values for the system parameters are in Table 1.

Table 1. System Parameters

Parameters	Values	Units
Link Inertia - J_l	9.3×10^{-3}	$kg \cdot m^2$
Motor Inertia - J_m	3.7×10^{-3}	$kg \cdot m^2$
Torsional Spring Constant - k	1.8×10^{-1}	$N \cdot m/rad$
Link Mass - m	2.1×10^{-1}	Kg
Link Length - l	0.15	m
Viscous Friction Coefficient -b_m	4.6×10^{-2}	$N \cdot m/V$
Gravity Constant - g	9.8	m/s^2
Amplifier Gain - k_τ	8×10^{-2}	Nm/V

The control input signal is the torque by the motor $k_\tau \cdot u = T_m$. The evaluation of the proposed method was performed by running K=100 simulations for a window length N+1, where $N \in \{2, 4, 6, 8, 10\}$, fitted with a sampling time of $t_s = 0.05s$ and a total time of each simulation as $T = 120s$. A measurement noise vector η_t was randomly generated for the following standard deviation values: {0, 0.01, 0.03, 0.05, 0.07, 0.1}. For a better observation of the mode estimation effect and of the algorithm capability, trajectory switches that occur every 20 s are added to the algorithm.

The coefficient μ and the tolerance for the stopping criteria have been chosen as 10^{-3} and 10^{-6}, respectively, in all the simulations. As for the noise corrupting measurement matrix initialization, the measurement noise covariance is $P_f = 10^{-4}$.

We consider a simulation scenario where the true initial state is set at $x_0 = [\pi,\ 0,\ \pi,\ 0]^T$. The sequence of the input signal of the system $\{u_t\}$ is generated as $u_t = 2\sin(2t)$, as shown in Fig. 3.

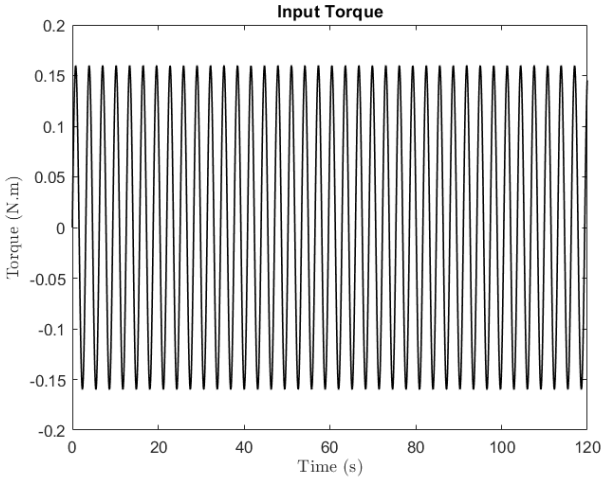

Fig. 3 System input signal.

For the sake of brevity, we refer to the estimator obtained by applying **Algorithm 1** as the moving-horizon estimation for switching system, where all the simulations have been performed in MATLAB on a computer equipped with a 1.99-GHz Intel i7 CPU and 16 GB of RAM. In particular, optimization has been performed through the nonlinear least-squares solver algorithm available within the routine *lsqnonlin* of the MATLAB Optimization Toolbox.

5. RESULTS

The simulation results showcased in Figures 4 to 12 illustrate the rigorous analytical framework stated in Section 1. Different values for the estimation horizon N have been taken into account in this study, as mentioned in the previous section. However, the first four plots refer only to the case of N = 10 (best case), even if similar plots could be displayed also for N = 2, 4, 6 and 8. In the sequence, we show the boxplot for the other window lengths.

Figures 4 and 5 compares the real and estimated continuous-time state of the position (x_1, x_3) and velocity (x_2, x_4). This values are obtained by means of MHE for N = 10 with a random noise standard deviation of $\sigma_\eta = 7.10^{-2}$. Note that the estimate appears to perfectly achieve the real position and velocity.

The real and estimated discrete-time modes are shown in Fig. 4 for the case where N = 10 and $\sigma_\eta = 7.10^{-2}$.

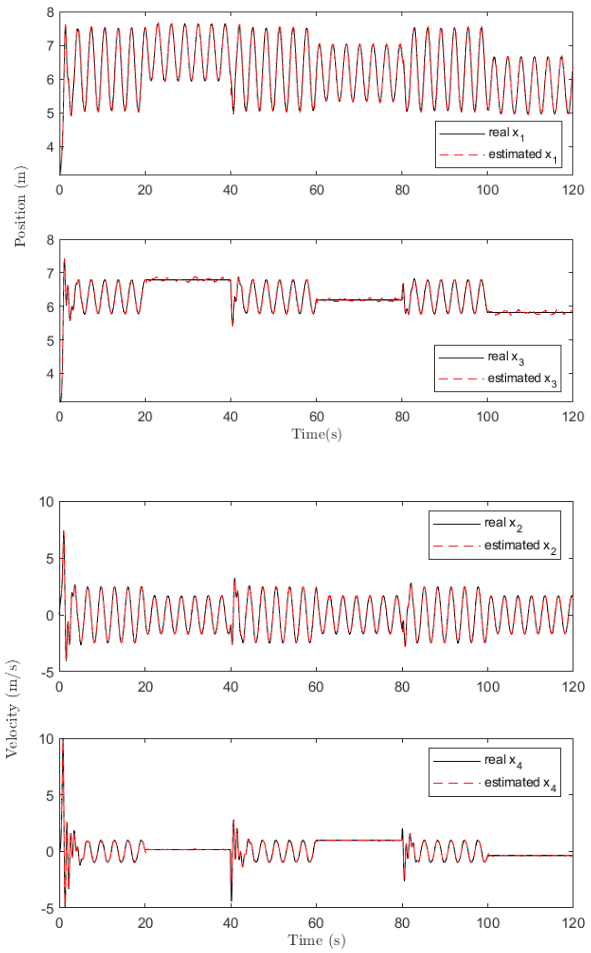

Fig. 4 Real value and estimates for the MHSE in the presence of noise with $\sigma_\eta = 7.10^{-2}$ and N = 10.

The solution of equation (11), illustrated in Fig 6, depict the percentage of correct mode estimations done at each time instant assuming the noise with $\sigma_\eta = 7.10^{-2}$, considering all K simulations.

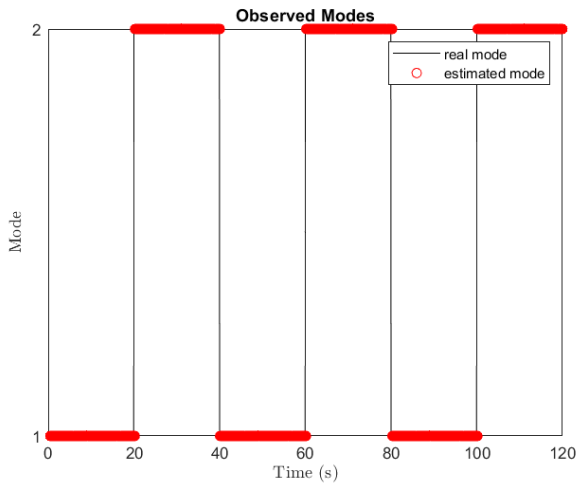

Fig. 5 Real modes and estimates for the MHE in the presence of noise with $\sigma_\eta = 7.10^{-2}$ and N = 10.

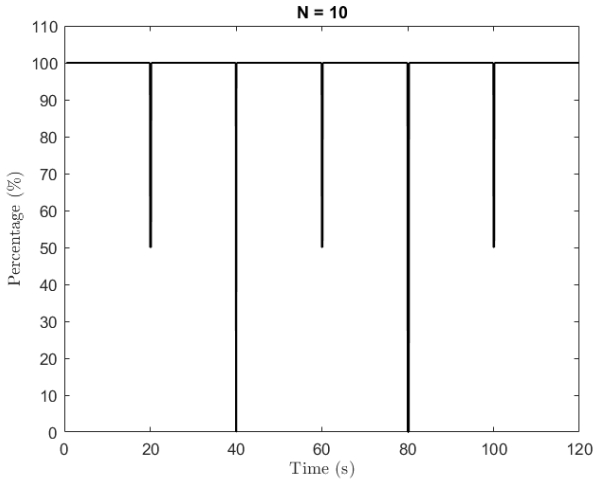

Fig. 6 Percentage of correct mode-estimation for fixed times in the presence of noise with $\sigma_\eta = 7.10^{-2}$ and N = 10.

Fig. 7 presents the plot of the RMSE, computed over 100 simulations, for the MHE in the presence of noises. The state estimation performance index shows that the difference between the real state and its estimate tends asymptotically to a small value in between switches, as is being confirmed by Fig 7.

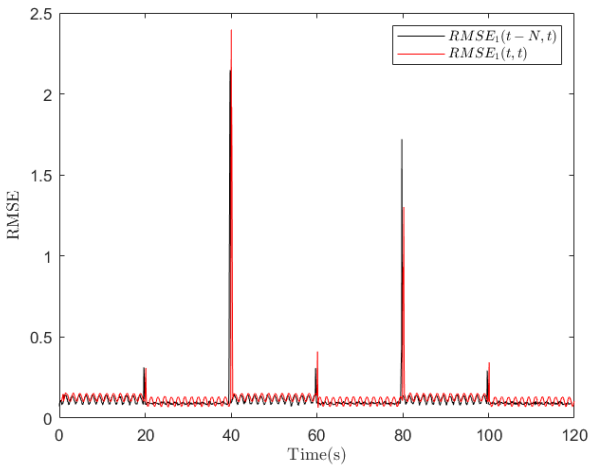

Fig. 7 RMSEs of the MHE in the presence of noise with $\sigma_\eta = 7.10^{-2}$ and N = 10.

Fig. 5, 6 and 7 show that the signal can reconstruct the mode with small errors perfectly in-between switches. However, around the switches of the mode (at 20 s, 40 s, 60 s, 80 s and 100 s) the mode estimation is not perfectly accurate. This is due to the fact that the mode is constant only within a given window (Ayala, 2012). Therefore, the given moving-horizon window length (N = 10) cannot properly be used to estimate the mode in one of the switching times.

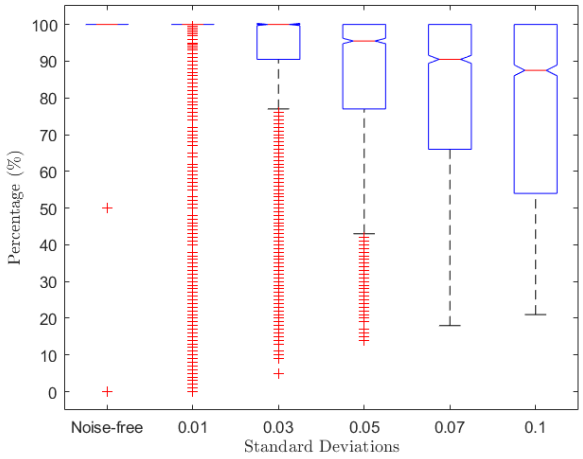

Fig. 8 Boxplots for the percentage of correct estimation of the modes for different levels of noise in N = 2.

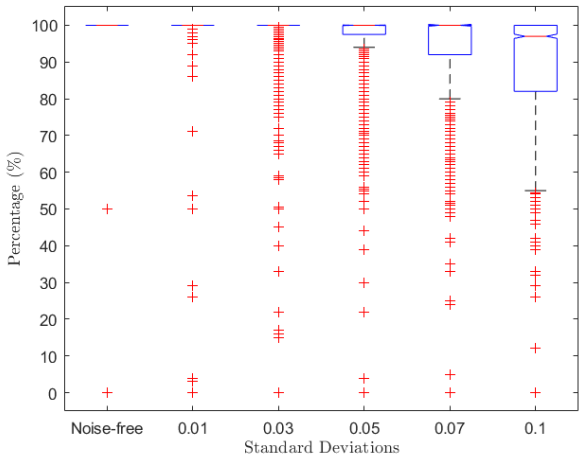

Fig. 9 Boxplots for the percentage of correct estimation of the modes for different levels of noise in N = 4.

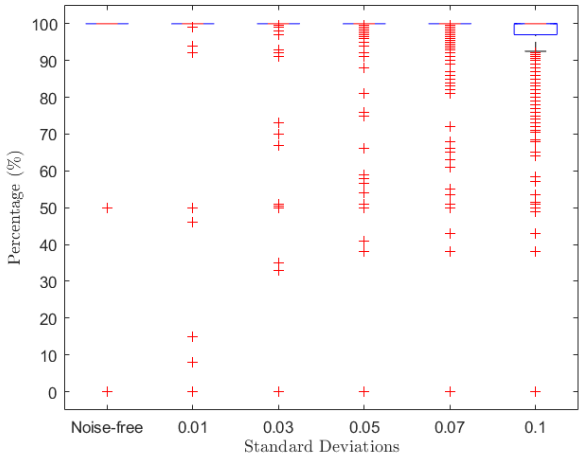

Fig. 10 Boxplots for the percentage of correct estimation of the modes for different levels of noise in N = 6.

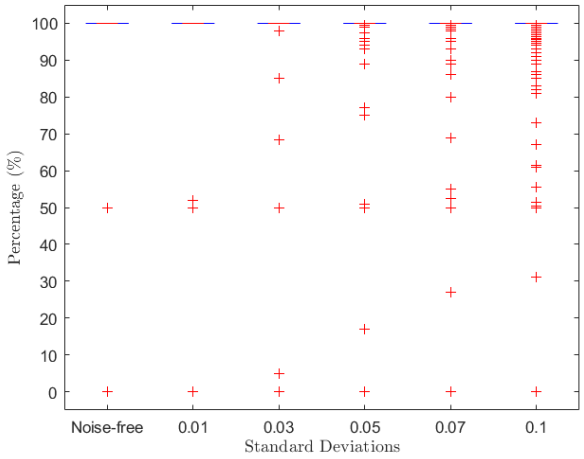

Fig. 11 Boxplots for the percentage of correct estimation of the modes for different levels of noise in N = 8.

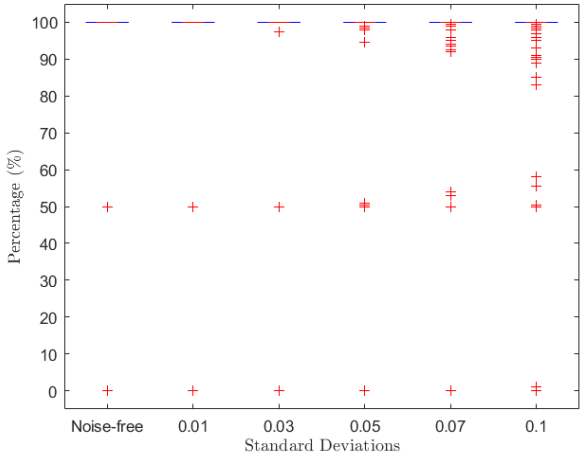

Fig. 12 Boxplots for the percentage of correct estimation of the modes for different levels of noise in N = 10.

Figures 8 to 12 and Table 2 summarizes the boxplots of the percentage of total correct mode estimations where each box represents the data for different standard deviation. In this work, the boxplot whiskers (in red) represent the outliers that are the observations below the half-lines, that is, observations that are out of the pattern observed in the data. Table 2 contains the medians shown in the boxplots for all assumptions of N and noise levels. The main idea behind those plots is to generate a sensibility analysis that shows how the results of the percentage of correct estimation improves in quality when the length of the horizon window N increases. Also, we expect the horizon window to be as small as possible.

Table 2. Median of the percentage of correct estimation of the modes

Noises St. Dev.	0	0,01	0,03	0,05	0,07	0,1
N+1 = 3	100	100	100	95,5	90,5	87,5
N+1 = 5	100	100	100	99,9	99,7	97
N+1 = 7	100	100	100	100	100	99,9
N+1 = 9	100	100	100	100	100	100
N+1 = 11	100	100	100	100	100	100

The simulations show that the MHE can reconstruct the mode perfectly once the percentage of correct mode estimations increase successively by increasing the length of the window N. This fact indicates that the mode estimation procedure becomes more robust, even if the noise affecting the observations increases. Fig. 8 and 12 show that, while for N = 2 the mode estimation is a quasi-random procedure when considering noises with standard deviation $\sigma_\eta = 7.10^{-2}$ and 10^{-1}, for N = 10 the noise affecting the system is practically fully filtered.

6. CONCLUSION

In this paper, we have investigated moving horizon estimators to detect contact in a single-link flexible joint manipulator. The manipulator is modeled as a switching discrete-time nonlinear system for which the challenge lies in the simultaneous discrete and continuous state and mode estimation. The main difficulty is how to set the observability parameters capable of estimating the mode and state of the switching nonlinear systems most effectively, with great accuracy, and low computational cost. This issue is addressed by performing the rigorous analytical framework proposed for the switching nonlinear systems and by investigating the times to run the simulations. By applying such properties, the performance of the proposed MH estimator is analyzed. Numerical example is provided to illustrate the solutions.

Future work will concern the extension of the approach to real-time application, where the efforts will be in performing a faster state estimation in an even more evident way. Online and offline estimation for switching nonlinear systems will be considered as well.

ACKNOWLEDGMENT

The authors gratefully acknowledge that this study was financed in part by the Coordenação de Aperfeiçoamento de Pessoal de Nível Superior - Brasil (CAPES) - Finance Code 001, and by the Department of Mechanical Engineering of the Pontifical Catholic University of Rio de Janeiro.

REFERENCES

Alessandri, A., Baglietto, M., Battistelli, G., & Zavala, V. (2010, December). *Advances in moving horizon estimation for nonlinear systems*. In 49th IEEE Conference on Decision and Control (CDC) (pp. 5681-5688). IEEE.

Alessandri, A., Baglietto, M., & Battistelli, G. (2005). *Receding-horizon estimation for switching discrete-time linear systems*. IEEE Transactions on Automatic Control, 50(11), 1736–1748.

Ayala, H. V. H. (2012). *Mode-observability of Nonlinear Switching Systems*. Master Thesis. University of Genova and Warsaw University of Technology. Unpublished.

Baglietto, M., Battistelli, G., Ayala, H. V. H., & Tesi, P. (2012, December). *Mode-observability conditions for linear and nonlinear systems*. In 2012 IEEE 51st IEEE Conference on Decision and Control (CDC) (pp. 1941-1947). IEEE.

Chen, Z., Wang, M., & Zou, Y. (2018). *Dynamic learning from adaptive neural control for flexible joint robot with tracking error constraints using high-gain observer*. Systems Science & Control Engineering, 6(3), 177-190.

Dimeas, F., Avendaño-Valencia, L., & Aspragathos, N. (2015). *Human - robot collision detection and identification based on fuzzy and time series modelling*. Robotica,33(9),1886-1898.doi:10.1017/S0263574714001143

Du Y, Liu F, Qiu J, Buss M..(2021) *A novel recursive approach for online identification of continuous-time switched nonlinear systems*. Int J Robust Nonlinear Control.31:7546–7565.https://doi.org/10.1002/rnc.5702

Fan, X., & Arcak, M. (2003). *Observer design for systems with multivariable monotone nonlinearities*. Systems & Control Letters, 50(4), 319-330.

Guo, Y., & Huang, B. (2013). *Moving horizon estimation for switching nonlinear systems*. Automatica, 49(11), 3270-3281.

Jung, B. J., Koo, J. C., Choi, H. R., & Moon, H. (2014). *Human-robot collision detection under modeling uncertainty using frequency boundary of manipulator dynamics*. Journal of Mechanical Science and Technology, 28(11), 4389-4395.

Kouris, A., Dimeas, F., & Aspragathos, N. (2018). *A frequency domain approach for contact type distinction in human–robot collaboration*. IEEE robotics and automation letters, 3(2), 720-727.

Li, Z. J., Wu, H. B., Yang, J. M., Wang, M. H., & Ye, J. H. (2018). *A position and torque switching control method for robot collision safety*. International Journal of Automation and Computing, 15(2), 156-168.

Liberzon, D. (*2003*). *Switching in Systems and Control*. Birkhauser.

Nocedal, J., & Wright, S. (2006). *Springer series in operations research and financial engineering. In Numerical optimization*. New York: Springer.

Ullah, H., Malik, F. M., Raza, A., Ahmad, I., Mazhar, N., & Khan, R. (2021, January). *Tracking control of flexible joint single link robotic manipulator via extended high-gain observer*. In 2021 International Bhurban Conference on Applied Sciences and Technologies (IBCAST) (pp. 630-635). IEEE.

Vorndamme, J., Schappler, M., & Haddadin, S. (2017, May). *Collision detection, isolation and identification for humanoids*. In 2017 IEEE International Conference on Robotics and Automation (ICRA) (pp. 4754-4761). IEEE.

Zhang, X., Polycarpou, M. M., Parisini, T. (2010). *Fault diagnosis of a class of nonlinear uncertain systems with Lipschitz nonlinearities using adaptive estimation*. Automatica, v. 46, n. 2, p. 290-299.